研究論文

Coherent Magnetic Fluctuations of Ergodized ELMy H-Mode in the JFT-2M Tokamak

LIU Wandong[1,2], MIURA Yukitoshi*[1] and JFT-2M Group[1]
[1] *Japan Atomic Energy Research Institute, Ibaraki 319-1106, Japan*
[2] *University of Science and Technology of China, Hefei, Anhui 230027, China*

(Received 12 January 1998/Accepted 6 May 1998)

Abstract

On the JFT-2M tokamak, the edge localized mode (ELM) induced by an external ergodic magnetic field is reproducibly obtained. After several single pulses, ELM behaves as bundles (3 or more bursts). Within one ELM, several separated bursts of magnetic fluctuations are observed. A statistical analysis shows that there are two kinds of coherent modes. One is a fixed low frequency mode which exists for all events and all shots. Another is a high frequency wide-spectrum mode which occurs only at the second magnetic burst. Some properties of the coherent modes are described.

Keywords:
edge localized mode, coherent mode, magnetic fluctuations, ergodic magnetic field, tokamak

1. Introduction

The edge localized modes (ELMs), characterized by a sharply increasing in Hα signals, cause an enhanced particle and energy loss in tokamak H-mode discharges. The finite loss is proved to be useful for controlling the continuous impurity accumulation and density increase for a steady-state H-mode operation. There are mainly two kinds of ELM, depending on the net transport energy flux P_{sep} through the edge plasma (separatrix or last closed magnetic surface), type I and type III[1]. Type III ELM appears when P_{sep} is just above a power threshold of H-mode, P_{th}, and its repetition frequency decreases with P_{sep}. When P_{sep} is large enough type III ELM disappears. Contrast to type III, type I ELM appears at a high P_{sep}, and the higher P_{sep} makes the higher its repetition frequency. In ITER, an ELMy H-mode is considered to be a normal operational mode[2]. Actively controlling of ELMs in H-mode is a key issue for a steady-state ELMy H-mode operation. There are several ways to control ELM[3-8]. On the JFT-2M tokamak, an external ergodic magnetic field was successfully used to control the type III ELMs. By increasing the strength of the ergodic field, ELMy H-mode can be achieved in a wide range of net transport power P_{sep} [4,9]. By testing many configurations of three ergodic coil sets, it was found that the helical field component which has the toroidal mode $n \geq 4$ is effective to produce ELMs[10].

ELMs are believed to be MHD activities, which occurring at the edge plasma, causes a temporal deformation of the transport barrier for H-mode. Larger magnetic fluctuations are always found accompanying with ELMs on many devices[11-13], some of them appear as precursors and some as a result of ELM events. However, the mechanism of ELM and ELM controlling is far from clear. The coherent modes of magnetic fluctuations are observed in the JFT-2M ELMs. To understand the relationship between the effective mode of the external field and the mode of the magnetic fluctuations, the mode evolution and the location of ELM are fundamentally important. In this paper, the phenomena of the ELMs stimulated by external ergodic magnetic field are reported and the properties of the magnetic fluctuations are investigated by means of a statistical method.

*Corresponding author's e-mail: miura@naka.jaeri.go.jp
†この論文は第14回年会にて招待講演として発表されたものを論文化したものです.

2. General descriptions on the experiment

2.1 Experimental conditions

By means of applying an external ergodic magnetic field, type-III ELM (named as ergodized ELM) appears in a wide range of P_{sep} on the JFT-2M tokamak. The reproducibility of ELMs stimulated by ergodic field makes it easy to study the ELMs in detail. Here we focus on the behaviors of magnetic fluctuations associated with the stimulated ELM activities.

JFT-2M is the D-shaped divertor tokamak. In this experiment, it is operated in an upper single null divertor configuration with a major radius of 1.3 m, an average minor radius of 0.33 m, an ellipticity of 1.4, a triangularity of 0.33. The working gas is hydrogen. H-mode discharges are obtained by neutral beam injection with a total power of 1.0 MW. Ergodic field is applied at 550 ms, 150 ms before neutral beam injection. Since the value of edge safety factor has some effects on the ergodized ELMs[14], the toroidal field B_t and the plasma current I_p and thus the edge (5 mm inside the separatrix surface) safety factor q_s are kept unchanged in the experiment, $B_t = 1.02$ T, $I_p = 215$ kA and $q_s = 3.1$ respectively.

Two fast magnetic probes, one is fixed at $r = 0.3$ m and $z = 0.1$ m and the other can be radially moved from $r = 0.305$ m to $r = 0.255$ m at $z = -0.1$ m, are used to measure the poloidal magnetic field fluctuations. The position of $r = 0.255$ m is just outside the separatrix. They are separated with a toroidal angle $\Delta\phi = \pi/8$ and a poloidal angle $\Delta\theta = 2\pi/9$. The sampling time is 1 μs and so that the effective domain of frequency is up to 500 kHz.

2.2 Statistical method

To demonstrate the spatial coherency or the mode of magnetic fluctuations, a statistical analysis for coherency between the signals of the probes are employed. Taking $X(\omega)$ and $Y(\omega)$ as the Fourier transformations of the two probe signals, one can define the statistical cross-spectral density $h_{xy}(\omega)$, cross-amplitude spectrum $A_{xy}(\omega)$, cross-phase spectrum $\Psi_{xy}(\omega)$ and coherency spectrum $C_{xy}(\omega)$ by,

$$h_{xy}(\omega) = A_{xy}^2(\omega)\exp[i\,\Psi_{xy}(\omega)] = <X(\omega)\,Y^*(\omega)>, \quad (1)$$

$$C_{xy}(\omega) = |<X(\omega)\,Y^*(\omega)>| \,/\, |<X(\omega)><Y(\omega)>|^{1/2}, \quad (2)$$

where $<\ >$ represents an ensemble average. Coherent global modes can be determined if $C_{xy}(\omega) \sim 1$, and some information of the modes can be obtained from $\Psi_{xy}(\omega)$.

Time series signals are divided into time slices to form the statistical samples. According to the time related to ELM pulse, they are selected as the elements of different statistical ensembles. The elements in a statistical ensemble can be from several similar shots for a better and more general statistics. The length of time slices is chosen as 128 μs (128 points of data) and two adjacent slices are half overlapped. Thus in the context the temporal resolution is 64 μs and the frequency resolution is 7.8 kHz.

2.3 Properties of ergodized ELM and magnetic fluctuations

L-H transition occurs about 20 ms after the neutral beam heating and the first ELM appears about 30 ms afterwards. Figure 1 shows a typical shot for the ergodized ELMy H-mode. Figure 1(a) and (c) are Hα

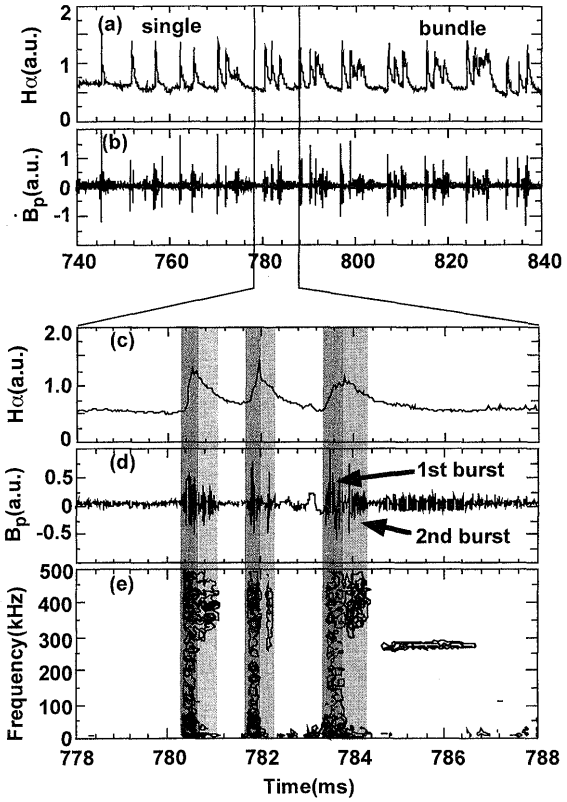

Fig. 1 Typical shot for the ergodized ELMy H-mode. (a) and (c) are Hα signals, (b) and (d) are magnetic fluctuations $\dot{B}_p$, and (e) is a contour plot for the amplitude of $\dot{B}_p$ spectrum.

signals which are the symbols of ELM phenomena, (b) and (d) are the magnetic fluctuations $\dot{B}_p$ picked by magnetic probes (in fact it is the time derivative of B_p), and (e) is a contour plot of the amplitude of B_p spectrum ($A_x = |X(\omega)|$). From the upper part of Fig. 1, one can see that after several single pulses, ELM behaves as bundles. There are 3 or more ELMs in a bundle. ELM burst has a short rising time (tens of μs) and a long decay time (~0.5 ms). The time between two single ELMs or bundle ELMs is more than 3 ms during which Hα signal can be completely recovered. But in a bundle, the succeeded ELM appears on the decay stage of the former one. They cannot be thought as independent each other. As shown in lower part of Fig. 1, there are two or more separated bursts of $\dot{B}_p$ associated with each ELM pulse. Since it lasts for a short time comparing with the decay time of Hα, the magnetic burst shows no much difference for different ELMs. The first magnetic burst begins at the same time of Hα rising within the uncertainty of the response time of Hα detectors (30 μs). The second magnetic burst appears about 50–100 μs after the first one ceases and lasts for 100–500 μs. Except the oscillations with very low frequency (< 2 kHz) in the last ELM in bundle or part of single ELM, no precursor magnetic fluctuations with higher frequency have been observed for this experiment.

As shown in Fig. 1(e), the main power of magnetic fluctuation is accumulated in two separated frequency domains. One is the low frequency (LF) domain (f < 50 kHz) and the other is the high frequency (HF) domain (f > 200 kHz).

3. Results of statistical analysis

3.1 Coherent Modes

Naturally, three statistical ensembles are analyzed, $\dot{B}_p$ between ELMs(E0), in the first bursts(E1) and in the second bursts(E2). Sometimes, ensemble E0 are divided into 4 sub-ensembles (E0-1 to E0-4) according to the time related to the beginning of the ELM, t = [0, −0.64], [−0.64, −1.28], [−1.28, −1.92] and [−1.92, −2.56] ms, respectively. Because the phase spectrum is found changing gradually during a shot, ensemble E2 is also divided into several sub-ensembles according to ELM number. For all the sub-ensemble of E0, although its amplitude is small the fluctuations have an obvious coherent LF mode (f < 40 kHz) with the coherency as high as 0.8. The cross-amplitude spectrum A_{xy} keeps at a low level for all the sub-ensembles. Figure 2(a) shows C_{xy}, A_{xy} and A_x for ensemble E1 in a typical shot. A_x has a sharp LF peak (f < 40 kHz) and

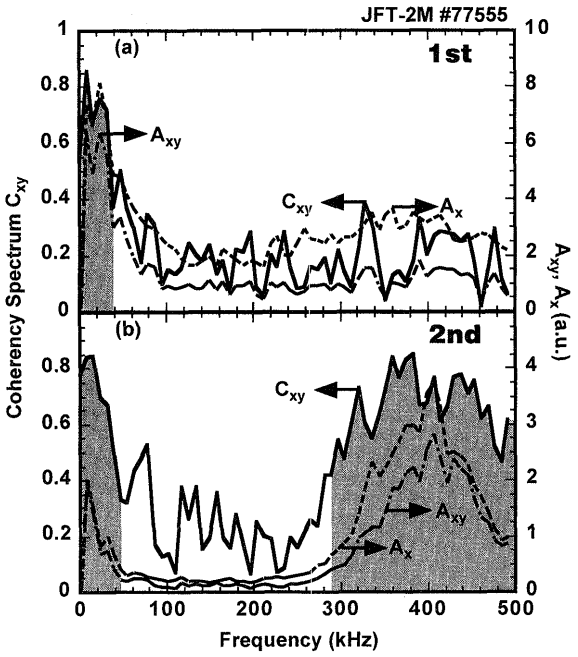

Fig. 2 Statistical coherency spectrum, cross-amplitude spectrum and amplitude spectrum of (a) the 1st and (b) the 2nd magnetic bursts in a shot. The coherent regions are shaded.

a wide HF peak (f > 300 kHz). From C_{xy} and A_{xy} one can see that the LF part is coherent and the HF part is incoherent. Figure 2(b) shows the case of ensemble E2. Although the LF part (f < 40 kHz) is still a coherent mode as before, its auto-power (A_x^2) of LF components is much smaller (about one order) than that in the 1st burst. The shape and value of the HF (f > 300 kHz) auto-power are not quite different from that in the 1st burst, but now the wide-spectrum HF components are coherent because of their large coherency (C_{xy} > 0.6).

The LF coherent mode keeps at a low level before ELM, sharply bursts at the beginning of ELM, and recovers to its original level soon after the 2nd burst. Since it always exists and its amplitude does not increase until the ELM begins, the LF coherent mode may not be considered directly as a precursor or a cause of ELM event, but it strongly correlates to the degrade of transport barrier, together with wide-spectrum incoherent HF fluctuations. There are two possible reasons for statistical incoherent results. One is that no fixed spatial modes exist (if there is, coherency should be high), and the other is that the mode number is very high so that it is really a localized or turbulent fluctuation. Because the 2nd magnetic bursts is on the decay stage of Hα, or the convalescence of transport

barrier, the coherent HF modes are linked to the establishment of the transport barrier rather than to its collapse.

3.2 Statistical phase spectrum and delay time

For a coherent mode, the statistical phase spectrum Ψ_{xy} is the statistical phase difference between the magnetic fluctuations at the two locations, $n\Delta\phi - m\Delta\theta$. Together with the safety factor of resonant layer q_{res}, the mode numbers (m, n) can be evaluated from Ψ_{xy}. A wide-spectrum coherent mode can be composed of some independent coherent modes. But if so, the value of phase spectrum in the coherent region is most possibly irregular because it is from different independent modes. In the experiment, it is found that for both the LF and HF coherent modes the phase spectrum in the coherent regions is a linear function of frequency. Figure 3 shows the statistical phase spectrum for different ensembles in LF region. Figure 3(a) shows Ψ_{xy} for six statistical ensembles (E0-1, E0-2, E0-3, E0-4, E1, E2) in a shot, and Fig. 3(b) shows Ψ_{xy} for ensemble E1 in different shots. In the incoherent region, the value of Ψ_{xy} widely spreads for different cases. But in the LF coherent region ($f < 40$ kHz), Ψ_{xy} increases linearly with frequency ($f = \omega/2\pi$) with a fixed slope of $\tau =$

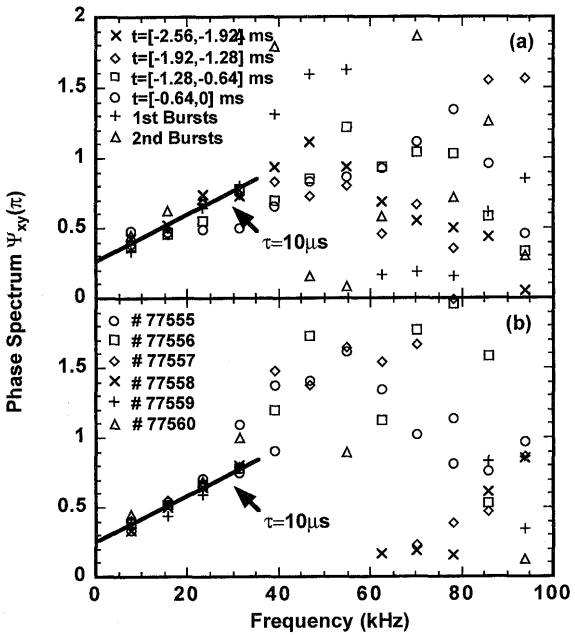

Fig. 3 Statistical phase spectrum of the LF coherent mode for (a) ensemble E0, E1 and E2 in shot 77558, and (b) ensemble E1 for different shots.

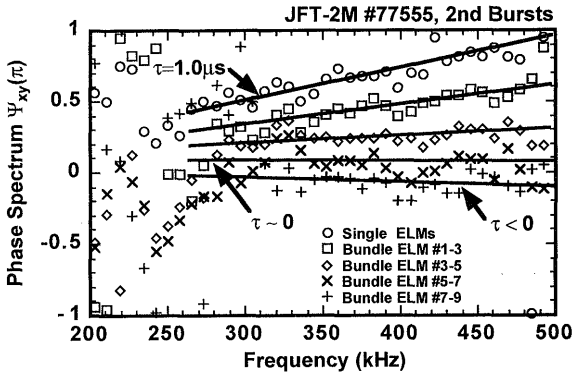

Fig. 4 Cross-phase spectrum of HF coherent modes and its evolution.

$\Delta\Psi_{xy}/\Delta\omega \sim 10$ μs for different statistical ensembles and for different shots. The slope of the line τ is the delay time between the two locations in which waves propagate from one to another. It supports that the LF coherent mode is the same for all cases. The linear relation of Ψ_{xy} with frequency also holds in the coherent HF mode for different sub-ensembles of E2, as shown in Fig. 4. The slope changes gradually from $\tau \sim 1$ μs to $\tau < 0$ as the statistics is taken from the earliest ELMs (single ELMs) to the latest ELMs (bundle ELM #7–9). $\Psi_{xy} \sim \omega\tau$ in a coherent region implies that the coherent mode has an unique propagation velocity for all the wave components.

3.3 Mode number

If the safety factor of resonant surface q_{res} is assumed the poloidal and toroidal modes (m, n) in the statistical sense can be determined from Ψ_{xy}, by

$$\Psi_{xy} = n\Delta\phi - m\Delta\theta + 2\pi i \qquad (i = \text{integer}), \quad (3)$$

and

$$q_{res} = m/n\,. \quad (4)$$

The main frequency at which A_{xy} gets its maximum is about 400 kHz and 20 kHz for the HF and LF mode, respectively. Ψ_{xy} decreases from 0.7π to -0.1π for the HF mode (see Fig. 4) and $\Psi_{xy} \sim 0.5\pi$ for the LF mode (see Fig. 3). Figure 5 is the diagram showing the possible combination (m, n) of the HF coherent mode. The thin solid and dashed lines are for $\Psi_{xy} \sim 0.7\pi$ and -0.1π, respectively. The constant slope of the lines is $\Delta\theta/\Delta\phi$. The thick lines are for the $q = 2$ and $q = 3$ surfaces. Assuming that the HF mode occurs at the edge region, ($q_{res} = 2 \sim 3$), the possible mode number (m, n) should be changed within shade windows. The central

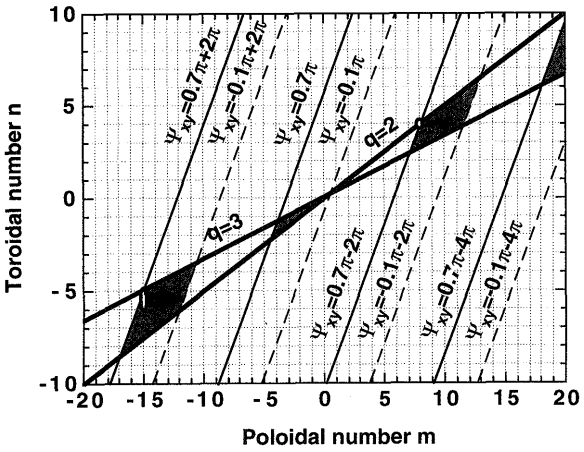

Fig. 5 Diagram for possible mode number of HF coherent mode and its evolution . The thin solid and dashed lines are for $\Psi_{xy} \sim 0.7\pi$ and -0.1π, respectively. The thick lines are for the $q = 2$ and $q = 3$ surfaces.

one where m is very low is not reasonable because it contains the origin ($m = 0$, $n = 0$). As shown by arrows in Fig. 5, the possible ways for mode evolution with lower mode numbers are, (i) $n = -5$ or -6 and the resonant layer moves inward (from $q_{res} \sim 3$ to $q_{res} \sim 2$); (ii) $n = 4$ and the resonant layer moves outward (from $q_{res} \sim 2$ to $q_{res} \sim 3$). Higher modes are also possible in the remain windows. However, we can get a conclusion that for HF coherent mode, $|n| \geq 4$.

For the LF mode, the line for $\Psi_{xy} \sim 0.5\pi$ is between the thin solid and dashed lines. Assuming that the LF mode also occurs at the edge region, ($q_{res} = 2 \sim 3$), the lowest toroidal number $n = -1$ is also possible since it is a fixed mode.

4. Conclusions

The ELMs stimulated by an external ergodic magnetic field for lower q discharge behaves as bundles after several separated single ELMs. Magnetic fluctuations show no much difference among the two kinds of ELMs. Generally, there are more than two bursts of magnetic fluctuations within an ELM. The power of fluctuations occupy two separated frequency regions, LF ($f < 50$ kHz) and HF ($f > 200$ kHz).

There are two coherent modes, LF ($f < 40$ kHz) and HF ($f > 300$ kHz). LF mode always exists and its phase spectrum keeps unchanged, which implies that it is a fixed mode, possible with a low mode number ($n = 1$). Wide-spectrum HF fluctuations are only coherent in the 2nd bursts. The delay time τ decreases with time. The resonant layer for HF mode moves during shot. If the resonant layer is at plasma edge ($q = 2 \sim 3$) the toroidal mode can be determined as $|n| \geq 4$, which is consistent with the effective modes of externally applied ergodic magnetic field to produce ELMs.

Acknowledgments

The authors would like to thank the members of JFT-2M team. Also, the authors acknowledge the arrangement of the movable magnetic probe with Drs. K. Hanada and S. Ohdachi. They also wish to express their gratitude to Drs. H. Kishimoto and M. Azumi for their continuous encouragement. This paper is dedicated for the memory of Dr. N. Suziki who led JFT-2M experiment for many years.

References

[1] H. Zohn, Plasma Phys. Control. Fusion **38**, 1213 (1996).
[2] D. Boucher *et al.*, Plasma Phys. Control. Fusion **38**, 1225 (1996).
[3] T. Shoji *et al,. Proc. 17th Europ. Conf. on Cont. Fusion & Plasma Phys.*, Amsterdam, Vol.**14B-3** (1990) p.1452.
[4] Y. Miura *et al., Plasma Physics and Controlled Nuclear Fusion Research 1991 (Proc. 13th Int. Conf. Washington)*, IAEA, Vienna Vol.**1** (1991) p.325.
[5] M. Dutch *et al.*, Nucl. Fusion **35**, 650 (1995).
[6] T.N. Todd *et al.*, Plasma Phys. Control. Fusion **35**, B231 (1993).
[7] A.W. Leonard *et al.*, Nucl. Fusion **31**, 1511 (1991).
[8] O. Gruber *et al.*, Phys. Rev. Lett. **74**, 4217 (1995).
[9] M. Mori, Plasma Phys. Control. Fusion **38**, 1189 (1996).
[10] M. Mori *et al., Plasma Physics and Controlled Nuclear Fusion Research 1993 (Proc. 14th Int. Conf. Wurtzburg)*, IAEA, Vienna Vol.**2** (1993) p.567.
[11] A.L. Colton *et al.*, Plasma Phys. Control. Fusion **38**, 1359 (1996).
[12] W. Suttrop *et al.*, Plasma Phys. Control. Fusion **38**, 1407 (1996).
[13] H. Zohn *et al.*, Nucl. Fusion **32**, 489 (1992).
[14] H. Tamai *et al., Plasma Physics and Controlled Nuclear Fusion Research 1995 (Proc. 15th Int. Conf. Seville)*, IAEA, Vienna Vol.**1** (1995) p.137.